

Downloaded via RICE UNIV on January 23, 2020 at 02:25:29 (UTC).  
See <https://pubs.acs.org/sharingguidelines> for options on how to legitimately share published articles.

Ammonium, a major nutrient, is commonly present in many waste streams, including municipal wastewater, livestock manure, and landfill leachate.<sup>16,17</sup> As the preferred nitrogen source for most bacteria,<sup>18</sup> ammonium addition is important for food waste fermentation to balance the high C/N ratio without introducing microbial competitors for LAB.<sup>19–21</sup> Furthermore, ammonium is involved in numerous processes in mixed culture reactors that can be generally divided into assimilation by LAB and other bacteria for anabolism and oxidation for catabolism by competing nitrifiers (with possible subsequent conversion to  $N_2$  by denitrification or anaerobic ammonium oxidation).<sup>18,22,23</sup> However, little is known about how ammonium addition impacts the LA fermentation pathway, the abundance of LAB, and key genes related to L-LA fermentation such as *ldhL*.

The activity of specific L-lactate dehydrogenase, responsible for L-LA production, has been reported to increase in a reducing environment (i.e., a lower oxidation–reduction potential, ORP).<sup>7,24,25</sup> Nevertheless, the role of ammonium in regulating the yield of highly optically active L-LA during FW fermentation has not been discerned. Thus, investigating the fate of ammonium during FW fermentation is important to optimize its usage and understand its limitations during the simultaneous recovery of valuable chiral molecules and nutrient removal from waste streams.

This study proposes a practical way to enhance L-LA production during FW fermentation through beneficial population and metabolic shifts stimulated by ammonium addition. FW fermentation was operated in repeated batch with no amendments (Ctrl), supplemented with autoclaved WAS (Org-N) or with ammonium (Am-N). A mechanistic insight is provided by comparing product spectra, microbiome structures, and metabolic functional genes and by quantifying ammonium transformation and fate via  $^{15}N$  isotope tracing. A relationship between pyruvate reduction and ammonium oxidation is explored along with correlations between ORP and L-LA yield, informed by quantification of key LAB genera and functional genes. Finally, the impact of ammonium addition on intracellular nicotinamide adenine dinucleotides ( $NAD^+$  and  $NADH$ , the direct electron donor for LA generation) levels is unveiled.

## MATERIALS AND METHODS

**Feedstock and Seed Reactor.** The WAS was withdrawn from the secondary sedimentation tank of the Shanghai Songjiang wastewater treatment plant (Shanghai, China) and concentrated by settling at 4 °C for 24 h. The main characteristics of the concentrated WAS were as follows: total suspended solids (TSS),  $15.59 \pm 1.27$  g/L; volatile suspended solids (VSS),  $9.80 \pm 0.89$  g/L; and total chemical oxygen demand (TCOD),  $13.97 \pm 1.01$  g/L. FW fetched from the First School Canteen of Donghua University was milled to a slurry state and diluted with tap water to make the characteristics as TSS  $125.60 \pm 6.40$  g/L, VSS  $123.76 \pm 5.25$  g/L, and TCOD  $130.02 \pm 6.69$  g/L. The treated WAS and FW were stored at 4 °C in a refrigerator prior to use. As shown in Table S1, Test 1, FW and WAS were mixed at a VSS ratio of 6:1 in the seed reactor (SR, 1000 mL working volume) as previously described,<sup>7</sup> adding tap water to dilute final TCOD to around  $40 \pm 1$  g/L. Then, SR was mechanically stirred (120 rpm) for 4 days at a temperature of  $35 \pm 1$  °C. Unless otherwise noted, the fermentation pH was intermittently adjusted to  $9.0 \pm 0.1$  (which favored alkaline hydrolysis and was reported to optimize lactate production<sup>26</sup>) using sodium hydroxide (10 M) or hydrochloric acid (3 M) every 6 h. In our preliminary study, the cofermentation of FW and nonautoclaved WAS (6:1 ratio) was operated in repeated batch (detailed in Supporting Information, Table S1, Test 2).

## Effect of Ammonium Dosage on Lactic acid Fermentation.

As shown in Table S1, Test 3, seven reactors were prepared containing 100 mL of inoculum from SR and 400 mL of fresh FW (TCOD 40 g/L), which were amended by  $NH_4Cl$  in different dosages: 0, 100, 200, 300, 400, 500, and 1000  $NH_4^+-N$  mg/L. Then, the reactors were operated for 4 days under the same conditions as SR. The contents of L-LA and D-LA were measured every day.

**Effect of Feed Strategy with Different Nitrogen Source on Lactic acid Production in Long-Term Repeated Batch Fermentation.** To evaluate the feed strategy in long-term fermentation, three kinds of reactors were provided with different nitrogen sources in Table S1, Test 4: (1) raw FW (reactor Ctrl); (2) FW supplemented with autoclaved WAS (6:1 VSS ratio, our system's optimum ratio for LA production<sup>7</sup>), representing organic nitrogen from WAS (reactor Org-N); and (3) FW added with ammonium (reactor Am-N). According to our preliminary study (Test 2), the addition of microbes from nonautoclaved WAS shifted the indigenous microbial community, which undermined the accumulation of LA. Thus, WAS was autoclaved at 121 °C for 30 min to prevent the interference of active microbes from WAS and still retain organic nitrogen in Org-N. Tap water was added to dilute the mixed substrates to make the final TCOD around  $40 \pm 1$  g/L in all reactors, containing a total carbohydrate concentration of  $28.3 \pm 1.5$  g COD/L. The optimal concentration of  $NH_4Cl$  in Am-N was 1146 mg/L, equal to 300 mg  $NH_4^+-N$ /L. The total Kjeldahl nitrogen (TKN) concentrations in both Org-N and Am-N reactors were similar, about  $791.5 \pm 28.6$  mg/L. Initially, three reactors containing 800 mL of corresponding substrate mentioned above were mixed with the same inoculum (200 mL) from SR. Every 4 days, 800 mL of fermentation mixture was withdrawn (residual 200 mL was retained) and replaced by 800 mL of corresponding fresh substrates. The repeated batch fermentation was operated in eight cycles for 32 days and conducted under the same conditions as SR.

The concentrations of L-LA, D-LA, VFA,  $NH_4^+-N$ ,  $NO_3^- -N$ ,  $NO_2^- -N$ , pyruvate, soluble proteins, and carbohydrates were assayed daily. To evaluate the efficiency of FW solubilization, the increase of soluble substrate ( $S_{COD}$ ) was recorded after one day in each cycle. The activities of the key enzymes relevant to hydrolysis (i.e.,  $\alpha$ -glucosidase and protease) were assayed after two days in each cycle. The activities of NAD-dependent lactate dehydrogenase (n-LDH, the enzyme responsible for LA production) and NAD-independent lactate dehydrogenase (i-LDH, converting LA into VFA) were recorded when the maximal LA was achieved.

**Microbial Community Structure Analyses.** Microbial community structure in SR, Ctrl, Org-N, and Am-N reactors was analyzed using 16S rRNA gene pyrosequencing. Samples were collected from SR, Ctrl, and Org-N after 3 days at the 4th and 6th cycles and Am-N at the 2nd, 4th, 6th, and 8th cycles. DNA was extracted immediately from these samples using the TIANamp Soil DNA Kit (Tiangen, Shanghai, China). The extracted DNA was amplified by the polymerase chain reaction using primers 338F (5'-ACTCCTACGG-GAGGCAGCA-3') and 806R (5'-GGACTACHVGGGTWTC-TAAT-3') in the V3–V4 region. Metagenomics sequencing was performed using an Illumina MiSeq system (Illumina MiSeq). The closest matching sequences were compared with reference sequences in the GenBank database of SILVA. Raw sequences were deposited in the NCBI Short Read Archive (SRA) database under accession numbers SRR7778918–SRR7778924 and SRR7778928–SRR7778931.

**$^{15}N$  Isotope Tracing.** Ammonia assimilation, ammonia oxidation, and denitrification were evaluated using the  $^{15}N$  isotope tracing technique, as shown in Table S1, Test 5. The pellets of the inoculum from Am-N were harvested by centrifugation and resuspended using Tris–hydrochloric acid (0.05 mol/L, pH 7.20), which was repeated 3 times to prevent the interference of  $^{14}N$  compounds from the indigenous fermentation substrate. The identical serum bottles (working volume 500 mL) were filled with 400 mL of FW (TCOD 40 g/L) and 100 mL of the washed inoculum from Am-N.  $^{15}NH_4Cl$  was added to one serum bottle ( $^{15}NH_4-R$ ) at 300 mg of  $^{15}NH_4^+-N$ /L. Then,  $^{15}NH_4-R$  was sealed with butyl rubber stopper after ultrasonic degas and argon blowing for 15 min to evacuate  $^{28}N_2$  from liquid and

headspace, and placed on a shaker for 4 days under the same condition as a seed reactor. Liquid samples were collected by filtration through a cellulose acetate filter with 0.45  $\mu\text{m}$  pore size for  $^{15}\text{NH}_4^+$ ,  $^{15}\text{NO}_3^-$ , and  $^{15}\text{NO}_2^-$  analysis through a gas isotope ratio mass spectrometer (Nu Instruments Ltd., Wrexham, U.K.). Solid samples were processed by vacuum freeze-drying after 3 times repeating centrifugation and resuspension to eliminate  $^{15}\text{N}$  interference from the residual liquid. The gas sample was eventually collected from the headspace for  $^{29}\text{N}_2$  and  $^{30}\text{N}_2$  analysis.

**Interaction of Pyruvate and Ammonium in Batch Fermentation.** Three serum bottles (labeled as  $\text{NH}_4\text{-R}$ ,  $\text{Py-R}$ , and  $\text{PyNH}_4\text{-R}$ ) were amended with different synthetic fermentation media (200 mL) and the same washed inoculum (20 mL) from Am-N according to Table S1, Test 6. The synthetic fermentation media contained 300 mg of  $\text{NH}_4^+\text{-N/L}$  (ammonium chloride) in  $\text{NH}_4\text{-R}$ , 1500 mg of pyruvate/L (sodium pyruvate) in  $\text{Py-R}$ , and both 1500 mg of pyruvate/L and 300 mg of  $\text{NH}_4^+\text{-N/L}$  in  $\text{PyNH}_4\text{-R}$ . To minimize the toxicity of free ammonia (FAN) to microorganisms, FAN was kept at a subinhibitory concentration ( $<3$  mg/L) by adjusting the pH to  $7.0 \pm 0.1$  using sodium hydroxide (3 M) or hydrochloric acid (3 M) every 6 h.<sup>27</sup> All other fermentation conditions were the same as described above. L-LA, D-LA,  $\text{NH}_4^+\text{-N}$ ,  $\text{NO}_3^-\text{-N}$ ,  $\text{NO}_2^-\text{-N}$ , and pyruvate were assayed after 4 days of fermentation for further electron balance.

**Analytical Methods.** Dissolved samples were prepared by filtration through a cellulose acetate filter with a pore size of 0.45  $\mu\text{m}$ . L- and D-LA were analyzed using a high-performance liquid chromatograph (HPLC, Thermo Scientific, UltiMate 3000) equipped with an Astec CLC-D (5  $\mu\text{m}$ , 15 cm  $\times$  4.6 mm) column and detected by UV (254 nm). Copper sulfate solution (5 mM) was used as mobile phase at a flow rate of 1.0 mL/min. The activities of protease,  $\alpha$ -glucosidase, n-LDH, i-LDH, VSS, VFA, pyruvate, soluble carbohydrates, soluble proteins,  $\text{NH}_4^+\text{-N}$ ,  $\text{NO}_3^-\text{-N}$ , and  $\text{NO}_2^-\text{-N}$  were determined according to our previous studies.<sup>24–26</sup> The ORP was monitored with an ORP meter. The C/N ratio of the substrate was calculated based on total carbon (TC) and total nitrogen (TN) contents that were determined by an elemental analyzer (Elementar Vario EL III, Germany).  $^{15}\text{N}$  tracer was analyzed by a gas isotope ratio mass spectrometer (Nu Instruments Ltd. Wrexham, UK) at Shanghai Engineering Research Center of Stable Isotope. The quantification of ammonia-oxidation- and denitrification-related genes were conducted via the quantitative polymerase chain reaction (qPCR) (details are given in the Supplementary Material). The intracellular concentrations of NADH and  $\text{NAD}^+$  were measured as previously described.<sup>28</sup>

**Optical Activity of L-LA (OA-L) Calculation and Statistical Analysis.** The optical activity of L-LA (OA-L) was defined as an enantiomeric excess value according to the following equation (eq 1),<sup>7</sup> where  $[L]$  and  $[D]$  were the concentrations of L- and D-LA, respectively.

$$\text{OA} - \text{L} (\%) = ([L] - [D]) / ([L] + [D]) \times 100\% \quad (1)$$

The repeated batch reactors (Ctrl, Org-N, and Am-N) were run in duplicate, and each treatment was repeated for eight cycles. Batch fermentation tests were carried out in triplicate serum bottles. All data were expressed as means  $\pm$  standard deviation (SD), and one-way analysis of variance (ANOVA) posthoc multiple comparison was adopted to determine whether differences between treatments were significant at the 95% confidence level. All statistical analyses were performed with SPSS 25.0. Electron balance calculations are detailed in the Supplementary Material.

## RESULTS AND DISCUSSION

**Addition of  $\text{NH}_4^+$  Significantly Increased L-LA Production and Optical Activity.** With the increase of  $\text{NH}_4^+\text{-N}$  dosage to 300 mg/L, the maximum LA production increased from 10.11 to 28.45 g COD/L and OA of L-LA enhanced from 38.20 to 59.40% (Table 1, time course detailed in Figure S3). Then, the maximum LA production stabilized at 31.24, 29.40, and 24.64 g of COD/L when 400, 500, and 1000

**Table 1. Effect of  $\text{NH}_4^+\text{-N}$  Dosage on LA Production and OA of L-LA<sup>a</sup>**

$\text{NH}_4^+\text{-N}$ (mg/L)	maximal lactic acid (g COD/L)	OA of L-lactic acid (%) <sup>a</sup>
0	10.11 $\pm$ 2.00	38.20 $\pm$ 5.72
100	19.66 $\pm$ 1.98	59.40 $\pm$ 3.97
200	18.73 $\pm$ 2.94	43.72 $\pm$ 3.19
300	28.45 $\pm$ 2.42	52.81 $\pm$ 4.64
400	31.24 $\pm$ 2.56	25.67 $\pm$ 2.28
500	29.40 $\pm$ 3.47	23.21 $\pm$ 3.16
1000	24.64 $\pm$ 2.23	15.41 $\pm$ 2.77

<sup>a</sup>The data reported were obtained when maximal LA was observed. The time courses are detailed in Figure S4.

mg of  $\text{NH}_4^+\text{-N/L}$  was added but OA of L-LA decreased to 25.67, 23.21, and 15.41%, respectively. Higher ammonium dosages might increase FAN concentrations, which can induce cell death.<sup>29–31</sup> Thus, the optimal  $\text{NH}_4^+\text{-N}$  dosage was set as 300 mg/L in the following repeated batch fermentation.

FW-repeated batch fermentation reactor Am-N, supplemented with 300 mg/L  $\text{NH}_4^+\text{-N}$ , had the highest LA production (24.49  $\pm$  3.56 g COD/L) and optically active L-LA yield (76.79  $\pm$  18.39%) (Figure 1a). Reactor Org-N, amended with autoclaved WAS (to exclude interference by WAS microbes), had the second-highest L-LA production (Figure 1b). Lactate rapidly accumulated in Org-N to the maximum level (20.94  $\pm$  3.21 g COD/L) in 3 days, with unstable L-LA yield (47.03  $\pm$  21.78%), but was then rapidly consumed. The lowest production of LA and lowest optically active L-LA yield (11.63  $\pm$  2.16 g COD/L and 16.79  $\pm$  5.98%, respectively) was observed in Ctrl, fed with only FW (Figure 1c). The production rate of D-LA in Am-N (0.72  $\pm$  0.28 g COD/(L day)) was lower than that in Org-N (1.68  $\pm$  0.42 g COD/(L day)) and Ctrl (1.02  $\pm$  0.22 g COD/(L day)) (Table S3), indicating that  $\text{NH}_4^+$  addition enhanced both the yield and optical purity of L-lactate fermentation. Previous methods to produce L-LA from FW resulted in 0.13–0.48 g/g TCOD (refers to substrate TCOD added) with optically active around 42–65%,<sup>8,25,26</sup> whereas our method was able to produce 0.54 g/g TCOD with 76.79  $\pm$  18.39% simply through the addition of ammonium. Note that this study is meant to provide proof of concept rather than optimize the L-LA yield. Further improvements may consider increasing the organic loading rate and hydrothermal or saccharification pretreatment of the raw substrate to increase L-LA accumulation.

**Addition of  $\text{NH}_4^+$  Alters the Fermentation Pathway To Improve Lactic acid Accumulation.** The crucial steps affecting LA accumulation during FW fermentation are solubilization, hydrolysis, glycolysis, and acidification.<sup>24</sup> During solubilization (Figure 2a), increases in the concentration of soluble substrates ( $S_{\text{COD}}$ ) were much higher in Org-N and Am-N reactors than in the unamended controls (Table S4,  $p < 0.05$ ). Clearly, ammonium amendment enhanced solubilization, which is essential for converting FW to readily available monomers in the hydrolysis stage. Subsequent hydrolysis of proteins to amino acids (measured by protease activity, Figure 2b) and polysaccharides to monosaccharides (measured by  $\alpha$ -glucosidase activity, Figure 2c) was enhanced in the following order of amendments: Org-N > Am-N > Ctrl (Table S4,  $p < 0.05$ ). This enhancement might be due to nitrogen addition shifting the C/N ratio (Table S5) to a favorable range for hydrolysis.<sup>32</sup> Moreover, carbohydrate removal rates in Am-N



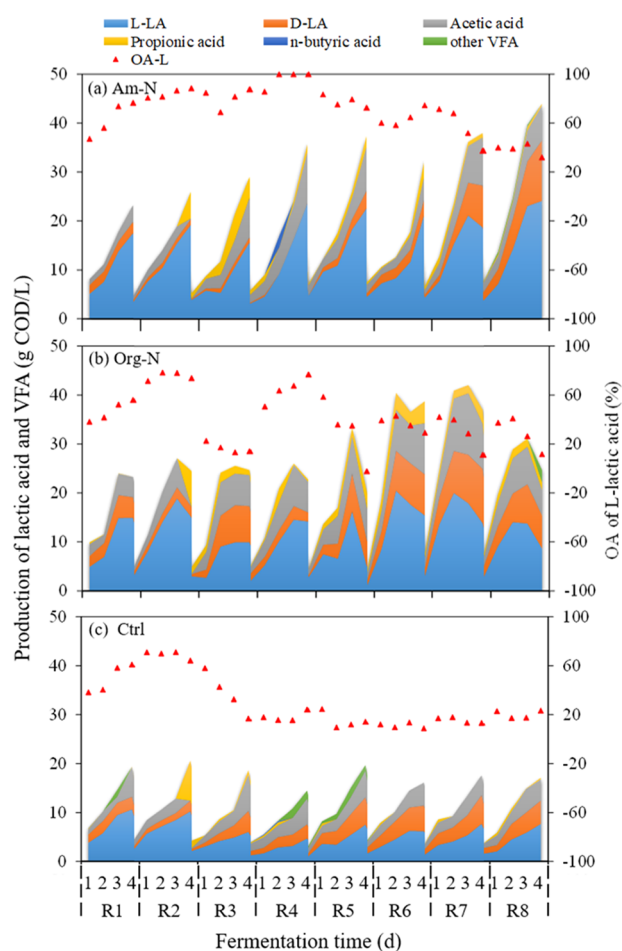


**Figure 1.** Lactic acid and volatile fatty acid (VFA) accumulation from food waste during long-term fermentation of Ctrl, Org-N, and Am-N. (a) Am-N with 300 mg/L  $\text{NH}_4^+\text{-N}$ , (b) Org-N with autoclaved sludge, and (c) Ctrl fed with only food waste. Red triangles represent OA-L. Average data are recorded in Figure S4, and statistical analysis is shown in Table S2.

( $4.63 \pm 0.74$  g COD/(L day)) and Org-N ( $5.17 \pm 1.18$  g COD/(L day)) reactors were significantly higher than those in unamended controls ( $1.38 \pm 0.96$  g COD/(L day)) (Figures 2d and S5a), indicating that glycolysis was stimulated by ammonium addition. This was followed by a higher accumulation of pyruvate in Org-N and Am-N (Figure S6).

Relative activities of n-LDH, the key enzyme responsible for LA generation from pyruvate, were higher in Am-N and Org-N than those in Ctrl reactors (Figure 2e) and so were LA production rates (Table S3). The relative activities of i-LDH (conversion of lactate into VFA) were significantly lower in Ctrl and Am-N compared to those in Org-N treatments (Figure 2f), which explains the higher VFA concentration in Org-N reactors ( $6.18 \pm 1.63$  g COD/L) versus that in Ctrl ( $6.18 \pm 1.63$  g COD/L) and Am-N ( $8.88 \pm 3.28$  g COD/L) (Figure 1). The main composition of VFA was acetic acid. Apparently, high abundance of proteins (from autoclaved WAS) in Org-N reactors (Figure S5b) stimulated protease activity (Figure 2b) and increased undesirable VFA production by providing amino acid substrates.<sup>33</sup> Adding ammonium directly (Am-N reactors) provides a nitrogen source without adding proteins that can be broken down into VFA substrates, leading to lower VFA production (Figure 1a). However, ammonium (less than 100 mg/L) was also generated via

deamination in Org-N (Figure S5c), which stimulated FW fermentation, resulting in higher lactate production than that in Ctrl but less than that in Am-N, which had 300 mg/L  $\text{NH}_4^+\text{-N}$  (Table 1 and Figure S3).

Ammonium consumption in both Am-N ( $\text{NH}_4^+\text{-N}$  decreased from 265.36 to 133.30 mg/L) and Org-N (from 62.07 to 12.24 mg/L) reactors (Figure S5c) was concomitant with increased LA production. The precise mechanisms by which FW solubilization, glycolysis, and L-LA production were enhanced by ammonium addition are confounded by the complexity of this system, and their discernment may require more reductionist studies. Nevertheless, the microbial community and functional gene analyses described below provide valuable insight into the nature of this enhancement.

**Addition of  $\text{NH}_4^+$  Increased the Relative Abundance of LAB and Enriched Key Functional Genes.** Microbial community structures in Ctrl, Org-N, and Am-N reactors varied greatly during long-term fermentation (Figures S7 and S8 and Table S6). At the genus level, *U\_F Flavobacteriaceae* (62.8%), a nitrogen-fixing bacterium,<sup>34</sup> was the largest group in Ctrl reactors (gray shadow in Figure 3a), indicating that nitrogen-fixing functions had evolved to meet the demand for N in this high C/N ( $31.1 \pm 4.2$ ) system. Samples from Ctrl, Org-N, and Am-N reactors had 19.4, 86.6, and 80.0%, respectively, of the total genus sequences associated with LA producing strains (blue shadow in Figure 3a).<sup>35–38</sup> This was in agreement with a higher LA concentration in Org-N and Am-N (Figure 1). The relative abundance of phylotypes, including *Streptococcus*, *Lactococcus*, *Enterococcus*, and *Corynebacterium*, that are most likely to produce L-LA<sup>35,36</sup> is higher in Am-N (42.2%) compared to that in Ctrl (5.3%) and Org-N (12.8%), which is consistent with higher OA of LA in Am-N (Figure 1). Especially, *Enterococcus* and *Corynebacterium*, dominated in Am-N are capable of surviving in a high ammonium environment.<sup>39,40</sup> Note that some LABs have both genes (*ldhL* and *ldhD*) encoding NADH-dependent L- and D-lactate dehydrogenases (L-LDH and D-LDH), respectively, responsible for L- and D-lactate generation.<sup>41</sup> Consistent with the observed yields of optically active L-LA (Figure 1), the relative abundance of *ldhL* was much higher in Am-N than that in Ctrl and Org-N reactors, whereas *ldhD* was lower in Am-N than that in Org-N treatments (Figure 3b). Furthermore, the relative abundance of key LAB genera (i.e., *Bavariicoccus*, *Bifidobacterium*, *Enterococcus*, and *Corynebacterium* in Figure 3c) was significantly correlated ( $p < 0.05$ ,  $R^2 = 0.94$ ) to that of *ldhL* (Figure 3c).

Differences in the abundance of functional genes can be assessed based on the KEGG database.<sup>42</sup> Key genes related to membrane transport (ABC transporters and permeases) and carbohydrate metabolism (particularly, pyruvate metabolism and glycolysis) were more abundant in Am-N and Org-N than Ctrl reactors (Figure S9), which is consistent with the improved fermentation activities (Figure 2). Since synthesizing the carrier protein such as permeases requires a nitrogen source,<sup>43</sup> ammonium may facilitate substrate uptake in the transport chain. In contrast, scarcity of ammonium in Ctrl reactors likely led to lower substrate transport into cells, limiting lactate metabolism.

#### <sup>15</sup>N Isotope Tracing during LA Fermentation.

Ammonium concentrations decreased from  $265.36 \pm 5.34$  to  $133.30 \pm 30.30$  mg/L in Am-N reactors, while nitrate levels increased from  $9.38 \pm 0.82$  to  $46.62 \pm 3.91$  mg/L without nitrite accumulation (Figure 4a). In Org-N reactors,

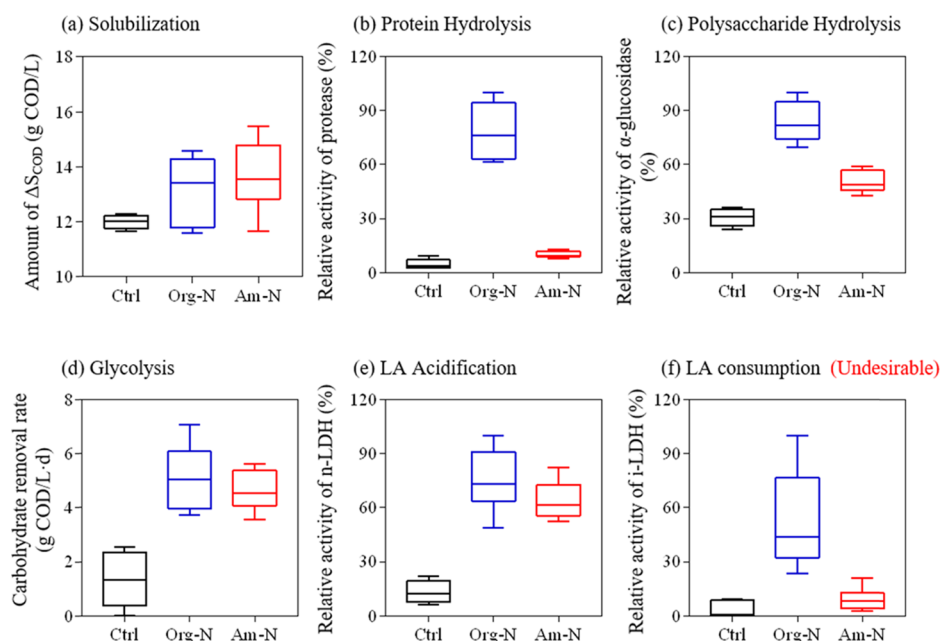


**Figure 2.** Solubilization, hydrolysis, glycolysis, and acidification in repeated batch fermentation of Ctrl, Org-N, and Am-N. (a) Soluble COD released ( $\Delta S_{COD}$ ) after 1 day of fermentation; the relative activities of key hydrolases, (b) protease and (c)  $\alpha$ -glucosidase, at 2 days of fermentation; (d) soluble carbohydrate reduction rate during the fermentation; and the relative activities of key enzymes related to (e) relative activity of n-LDH (LA production) and (f) i-LDH (undesirable LA consumption) at 3 days of fermentation. Each box plot shows minimum (error bar), maximum (error bar), first quartile, median, third quartile, and maximum values from the data of eight cycles, which are detailed in the [Supplementary Material](#).

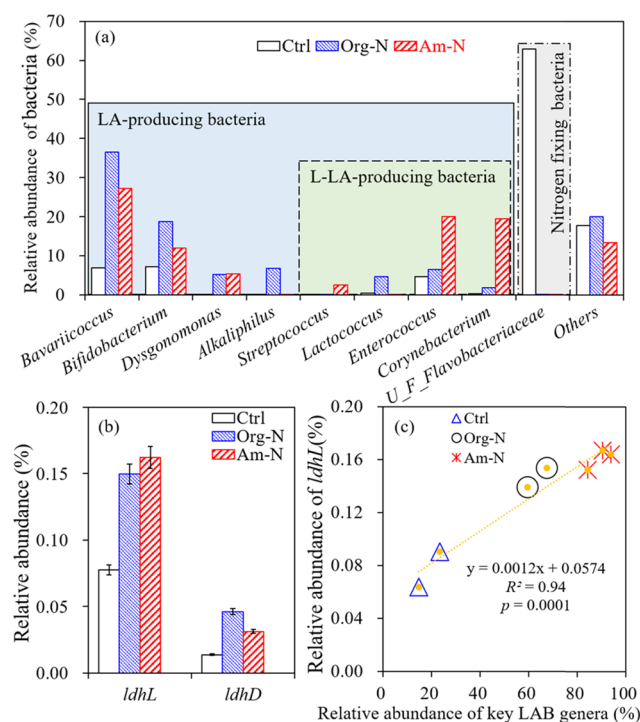


**Figure 3.** Selected genotypes and functional genes in the repeated batch fermentation of Ctrl, Org-N, and Am-N. (a) Relative abundance of LAB and denitrifiers at genus levels (taxonomic details are in [Figures S7 and S8](#)), (b) relative abundance of functional genes (*ldhL* and *ldhD*), and (c) regression analysis of the correlation between key LAB genera and abundance of *ldhL*.

ammonium first peaked at  $62.07 \pm 10.52$  mg/L due to deamination<sup>44,45</sup> and then decreased to  $12.24 \pm 7.05$  mg/L,

while nitrate accumulated from  $9.86 \pm 0.59$  to  $49.49 \pm 2.78$  mg/L. In Ctrl reactors, ammonium and nitrate both slightly increased to 24.26 and 23.58 mg/L during fermentation.

Ammonium transformations were further quantified by  $^{15}\text{N}$  isotope tracing in a reactor fed with FW and  $^{15}\text{NH}_4\text{Cl}$  ([Figure 4b](#)). However, the consumption of  $^{15}\text{NH}_4\text{Cl}$  in this reactor was only 30.8% ([Figure S10](#)) compared to an average consumption of 49.8% in Am-N reactors ([Figure S5c](#)). This is likely due to the isotopic fractionation effect, where lighter  $^{14}\text{N}$  atoms are utilized at a higher rate than  $^{15}\text{N}$ .<sup>46</sup> About one-half of the ammonium consumption was attributed to assimilation since 46.6% of the utilized  $^{15}\text{NH}_4\text{Cl}$  was associated with biomass versus 15.3% oxidized to  $^{15}\text{NO}_3^-$ -N and 31.0% to  $^{29}\text{N}_2$  and  $^{30}\text{N}_2$  ([Figures 4b and S10](#)). The KEGG pathway database indicates that the relative abundance of functional genes related to ammonia assimilation (GOGAT) was higher in Am-N and Org-N than that in Ctrl reactors ([Figure S11](#)).

**Mechanistic Insight into the Role of Ammonium-Stimulating LA Production with High OA-L.** Nitrogen is essential to synthesize carrier proteins for facilitated diffusion and active transport, with ammonium being one of the preferable nitrogen sources for all bacteria including LAB.<sup>18</sup> For example, the addition of ammonium enhanced substrate transport activities ([Figure S9](#)) and resulted in a higher concentration of pyruvate in Am-N ([Figure S6](#)), the precursor of LA. This is consistent with one-half of the added ammonium utilized for bacterial assimilation ([Figure 4b](#)), including LAB anabolism and proliferation ([Figure 3a](#)). On the other hand, we tested whether ammonium affects L-LA generation by coupling to pyruvate. In  $\text{PyNH}_4\text{-R}$  (synthetic media containing both pyruvate and ammonium), ammonium decreased from 300.3 to 168.8 mg/L ([Figure 5a](#)) and lactate production, OA of L-LA, and pyruvate consumption were all significantly higher than in the ammonium-free reactor (Py-R,

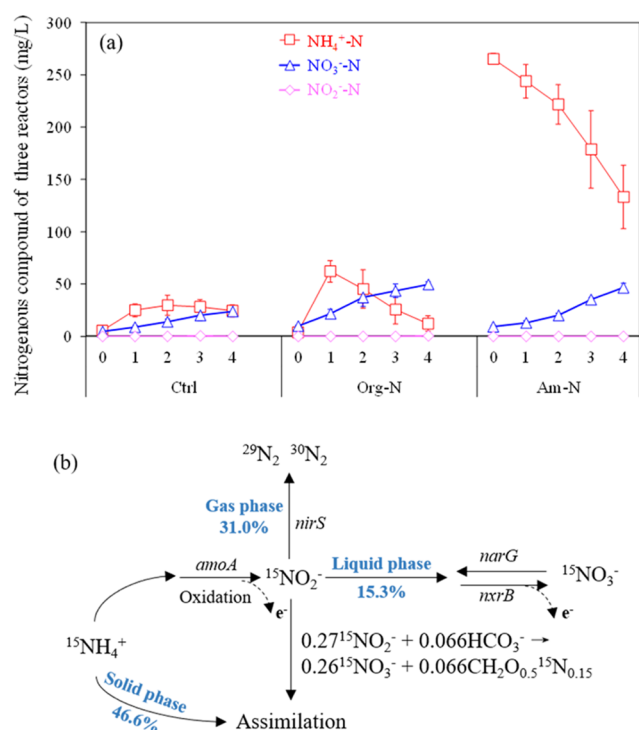


**Figure 4.** Nitrogen transformation during LA fermentation. (a) Average concentration of nitrogenous compounds (ammonium, nitrate, and nitrite) during one cycle of the fermentation stage in three repeated batch reactors. (b) Ammonium nitrogen fate analysis using  $^{15}\text{N}$  isotope tracing;  $^{29}\text{N}_2$  and  $^{30}\text{N}_2$  were probably originated from  $^{15}\text{N}$  nitrogen via ammonia oxidation to  $^{15}\text{NO}_3^-$  that was subsequently denitrified. Relative abundance of ammonia-oxidation-related genes (*amoA* and *nirB*) and denitrification-related genes (*narG* and *nirS*) is detailed in Figure S12 in the Supporting Information.

containing only pyruvate) (Figure 5b). No depletion of ammonium was observed in the absence of pyruvate ( $\text{NH}_4\text{-R}$ , containing only ammonium), indicating a strong link between pyruvate and ammonium in this simplified system. In this study, electrons derived from ammonia oxidation (21.28 mM) were a relatively small fraction of the electron donor pool

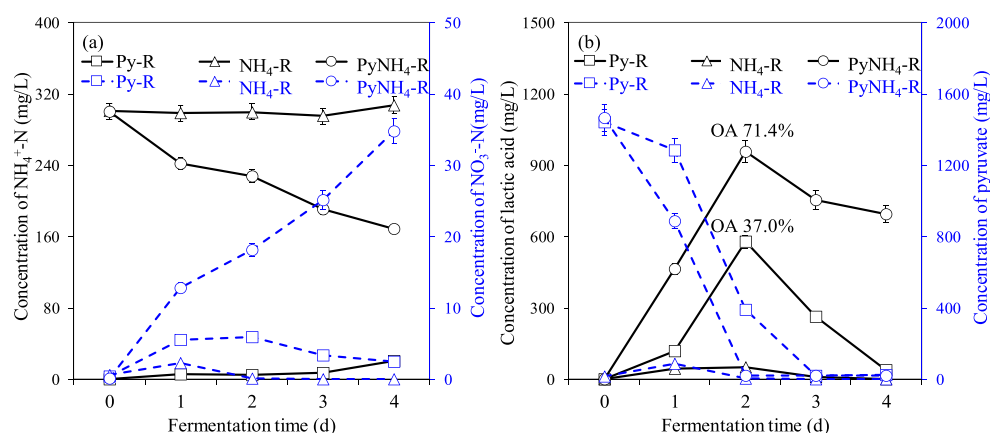


**Figure 5.** Lactate fermentation using synthetic medium amended with either pyruvate (Py-R) or ammonium ( $\text{NH}_4\text{-R}$ ) or both ( $\text{PyNH}_4\text{-R}$ ). (a) Variation of ammonia (solid line) and nitrate (dashed line) in Py-R,  $\text{NH}_4\text{-R}$ , and  $\text{PyNH}_4\text{-R}$  during the fermentation time course. Nitrite was not observed in three reactors. (b) Lactate generation (solid line) and pyruvate consumption (dashed line) in three reactors. OA was recorded when the maximal concentration of lactate was observed.

(510 mM electrons) and likely had minimal or no effect on L-LA production (Table S7).

Not only was ammonium assimilation associated with metabolic changes and bacterial population shifts but also a lower ORP and higher intracellular NADH levels. In the Ctrl, ORP continuously increased from  $-450$  to  $-200$  mV over time, whereas Am-N had a more stable reducing environment from  $-470$  to  $-320$  mV (Figure S13). The increased ORP tendency might be due to glycolysis and acidification processes,<sup>47</sup> which correspondingly consumed reducing substrates such as glucose and produced oxidative intermediate (i.e., lactate and acetate as shown in Table S8). In this study, the lower ORP was correlated ( $k = -0.2$ ,  $R^2 = 0.43$ ,  $p < 0.05$ ) with a higher OA of L-LA during long-term fermentation (Figure 6). Whereas correlation does not prove causation, we

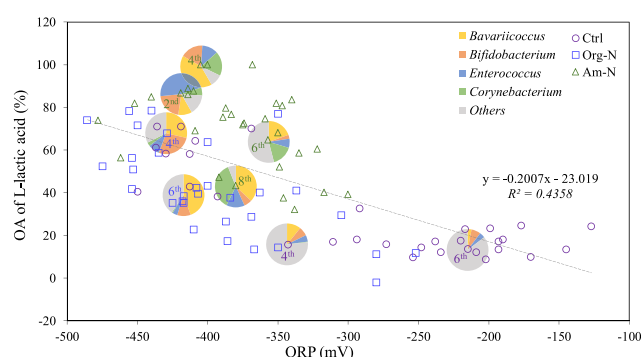


**Figure 6.** Linear regressions between ORP and OA-L in the repeated batch fermentation of Ctrl, Org-N, and Am-N, overlapped by key LAB genera. Variations of ORP along with fermentation time course are detailed in Figure S13. The positions of the overlapped circles, labeled in 2nd, 4th, 6th, and 8th cycles, correspond to the given pairs of OA-L and ORP when the bacteria samples were fetched out. The areas of the color sectors represent the relative abundance of the LAB genera from total bacteria that has a high correlation with *ldhL* (Figure 3c).

cannot rule out that low ORP may exert selective pressure for some specific L-LA producing genera (Figures 6 and S14) and enrich *ldhL* genes (Figure 3). It was reported that the extracellular ORP could impact intracellular redox homeo-



stasis, gene expression, and enzyme synthesis and consequently control profiles of fermentation products.<sup>47,48</sup> For example, a lower ORP resulted in an increase in LA production from glucose in anaerobic fermentation by *Klebsiella pneumoniae*.<sup>48</sup> Our recent study showed that OA of L-LA was significantly improved by providing a cathode applied with  $-100$  mV (a reducing environment) in cathodic electrofermentation of FW, which also resulted in a community shift toward phylotypes that are most likely to produce L-LA.<sup>25</sup> Additionally, lower ORP has also been reported to influence the  $\text{NAD}^+/\text{NADH}$  redox balance.<sup>49,50</sup> Thus, a higher intracellular NADH level was also observed in Am-N ( $0.46 \pm 0.02$  vs  $0.26 \pm 0.01$  mM for unamended controls,  $p < 0.05$ ) and the ratio of  $\text{NAD}^+/\text{NADH}$  almost doubled when ammonium was added (Figure 7). NADH is the direct electron donor linking the reduction of

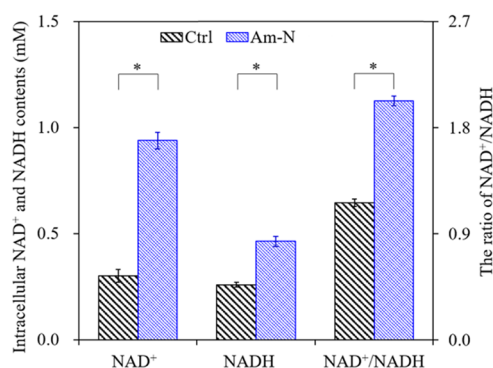


**Figure 7.** Comparison of intracellular  $\text{NAD}^+$  and NADH levels in Ctrl and Am-N. The higher ratio of  $\text{NAD}^+/\text{NADH}$  shows that most of NADH has taken part in bioreductive reactions in the cell as an electron donor, which is necessary for NADH regeneration in oxidative pathways. Statistical significance ( $p < 0.05$ ) of Ctrl and Am-N is indicated by asterisks (\*).

pyruvate to lactate,  $\text{pyruvate} + \text{NADH} + \text{H}^+ \rightarrow \text{lactate} + \text{NAD}^+$ , implying that a higher NADH level may increase the lactate yield rather than stereospecificity.<sup>41</sup> Furthermore, a higher ratio of  $\text{NAD}^+/\text{NADH}$  not only reflects the result of metabolic flux of the cell, indicating that more NADH underwent reductive reactions as electron donor,<sup>48</sup> but also enhances the activities of  $\text{NAD}^+$ -dependent enzymes,<sup>51</sup> increasing both the glycolysis step (Figure 2d) and NADH regeneration (Figure 7) in oxidative pathways, as proposed in Figure S15. Thus, ammonium addition resulted in a stable reducing environment (ORP ranged from  $-470$  to  $-320$  mV) and higher intracellular NADH levels, both possibly contributing to higher L-LA production.

## CONCLUSIONS

We propose a simple and practical approach for the valorization of FW during biological treatment, involving the addition of ammonium (300 mg/L) to enhance fermentation to a high value-added platform molecule (i.e., optically active L-lactic acid). This approach doubled the yield of L-LA and increased its optical activity by fivefold, which was attributed to a significant increase in the relative abundance of key LAB genera as well as a higher total abundance of the *ldhL* gene associated with pyruvate reduction to L-LA. Ammonium provided essential nitrogen for LAB growth and promoted a stable reducing environment that increased intracellular NADH levels for pyruvate reduction to L-lactate. Overall,

this study highlights ammonium as an overlooked biostimulator in mixed culture fermentation of organic waste to simultaneously enhance the resource recovery of valuable chiral molecules and nutrient removal from waste streams.

## ASSOCIATED CONTENT

### Supporting Information

The Supporting Information is available free of charge at <https://pubs.acs.org/doi/10.1021/acssuschemeng.9b06532>.

Analytic methods; electron balance calculation; statistical analysis; richness and diversity indexes; variation of soluble carbohydrate, proteins,  $\text{NH}_4^+\text{-N}$ , pyruvate, and ORP; distribution of bacterial communities; ammonia transformation; qPCR analysis and other reactor performance data (PDF)

## AUTHOR INFORMATION

### Corresponding Author

\*E-mail: [lix@dhu.edu.cn](mailto:lix@dhu.edu.cn). Tel: 86-21-67792538. Fax: 86-21-67792159.

### ORCID

Wenjuan Zhang: 0000-0002-8622-8414

Yanan Liu: 0000-0002-2582-7501

Pedro J. J. Alvarez: 0000-0002-6725-7199

### Notes

The authors declare no competing financial interest.

## ACKNOWLEDGMENTS

This work was supported by the Natural Science Foundation of China (NSFC) (51878137, 51878136, and 51878135); the Fundamental Research Funds for the Central Universities and the Donghua University Distinguished Young Professor Program; Shanghai Chen-Guang Program (17CG34); and the State Scholarship Fund of China under Grant 201806635006 from the China Scholarship Council.

## REFERENCES

- (1) Gunasekera, D. Cut food waste to help feed world. *Nature* **2015**, *524*, 415.
- (2) Liu, H.; Chen, Y. G. Enhanced Methane Production from Food Waste Using Cysteine To Increase Biotransformation of L-Monosaccharide, Volatile Fatty Acids, and Biohydrogen. *Environ. Sci. Technol.* **2018**, *52*, 3777–3785.
- (3) Kim, M. S.; Na, J. G.; Lee, M. K.; Ryu, H.; Chang, Y. K.; Triolo, J. M.; Yun, Y. M.; Kim, D. H. More value from food waste: Lactic acid and biogas recovery. *Water Res.* **2016**, *96*, 208–216.
- (4) Abdel-Rahman, M. A.; Sonomoto, K. Opportunities to overcome the current limitations and challenges for efficient microbial production of optically pure lactic acid. *J. Biotechnol.* **2016**, *236*, 176–192.
- (5) Tashiro, Y.; Kaneko, W.; Sun, Y.; Shibata, K.; Inokuma, K.; Zendo, T.; Sonomoto, K. Continuous d-lactic acid production by a noveltolerant *Lactobacillus delbrueckii* subsp. *lactis* QU 41. *Appl. Microbiol. Biotechnol.* **2011**, *89*, 1741–1750.
- (6) Klotz, S.; Kaufmann, N.; Kuenz, A.; Prusse, U. Biotechnological production of enantiomerically pure d-lactic acid. *Appl. Microbiol. Biotechnol.* **2016**, *100*, 9423–9437.
- (7) Li, X.; Chen, Y.; Zhao, S.; Chen, H.; Zheng, X.; Luo, J.; Liu, Y. Efficient production of optically pure L-lactic acid from food waste at ambient temperature by regulating key enzyme activity. *Water Res.* **2015**, *70*, 148–157.
- (8) Akao, S.; Tsuno, H.; Horie, T.; Mori, S. Effects of pH and temperature on products and bacterial community in L-lactate batch

fermentation of garbage under unsterile condition. *Water Res.* **2007**, *41*, 2636–2642.

(9) Li, J.; Zhang, W.; Li, X.; Ye, T.; Gan, Y.; Zhang, A.; Chen, H.; Xue, G.; Liu, Y. Production of lactic acid from thermal pretreated food waste through the fermentation of waste activated sludge: Effects of substrate and thermal pretreatment temperature. *Bioresour. Technol.* **2018**, *247*, 890–896.

(10) Zheng, J.; Gao, M.; Wang, Q.; Wang, J.; Sun, X.; Chang, Q.; Tashiro, Y. Enhancement of L-lactic acid production via synergism in open co-fermentation of *Sophora flavescens* residues and food waste. *Bioresour. Technol.* **2017**, *225*, 159–164.

(11) Zhao, J. W.; Zhang, C.; Wang, D. B.; Li, X. M.; An, H. X.; Xie, T.; Chen, F.; Xu, Q. X.; Sun, Y. J.; Zeng, G. M.; Yang, Q. Revealing the Underlying Mechanisms of How Sodium Chloride Affects Short-Chain Fatty Acid Production from the Cofermentation of Waste Activated Sludge and Food Waste. *ACS Sustainable Chem. Eng.* **2016**, *4*, 4675–4684.

(12) Li, X.; Zhang, W. J.; Ma, L.; Lai, S. Z.; Zhao, S.; Chen, Y. G.; Liu, Y. N. Improved production of propionic acid driven by hydrolyzed liquid containing high concentration of L-lactic acid from co-fermentation of food waste and sludge. *Bioresour. Technol.* **2016**, *220*, 523–529.

(13) Chen, Y.; Li, X.; Zheng, X.; Wang, D. Enhancement of propionic acid fraction in volatile fatty acids produced from sludge fermentation by the use of food waste and *Propionibacterium acidipropionici*. *Water Res.* **2013**, *47*, 615–622.

(14) Huang, L.; Chen, Z.; Xiong, D.; Wen, Q.; Ji, Y. Oriented acidification of wasted activated sludge (WAS) focused on odd-carbon volatile fatty acid (VFA): Regulation strategy and microbial community dynamics. *Water Res.* **2018**, *142*, 256–266.

(15) Tamis, J.; Joosse, B.; Loosdrecht, Mv.; Kleerebezem, R. High-rate volatile fatty acid (VFA) production by a granular sludge process at low pH. *Biotechnol. Bioeng.* **2015**, *112*, 2248–2255.

(16) Mahmoud, M.; Parameswaran, P.; Torres, C. I.; Rittmann, B. E. Fermentation pre-treatment of landfill leachate for enhanced electron recovery in a microbial electrolysis cell. *Bioresour. Technol.* **2014**, *151*, 151–158.

(17) Yenigün, O.; Demirel, B. Ammonia inhibition in anaerobic digestion: A review. *Process Biochem.* **2013**, *48*, 901–911.

(18) Kim, M.; Zhang, Z. G.; Okano, H.; Yan, D. L.; Groisman, A.; Hwa, T. Need-based activation of ammonium uptake in *Escherichia coli*. *Mol. Syst. Biol.* **2012**, *8*, 1–10.

(19) Mahmoud, M.; Torres, C. I.; Rittmann, B. E. Changes in Glucose Fermentation Pathways as a Response to the Free Ammonia Concentration in Microbial Electrolysis Cells. *Environ. Sci. Technol.* **2017**, *51*, 13461–13470.

(20) Wang, D. B.; Huang, Y. X.; Xu, Q. X.; Liu, X. R.; Yang, Q.; Li, X. M. Free ammonia aids ultrasound pretreatment to enhance short-chain fatty acids production from waste activated sludge. *Bioresour. Technol.* **2019**, *275*, 163–171.

(21) Wang, D.; Wang, Y.; Liu, X. R.; Xu, Q.; Yang, Q.; Li, X.; Zhang, Y.; Liu, Y.; Wang, Q.; Ni, B.; Li, H. Heat pretreatment assists free ammonia to enhance hydrogen production from waste activated sludge. *Bioresour. Technol.* **2019**, *283*, 316–325.

(22) Chen, X. M.; Guo, J. H.; Shi, Y.; Hu, S. H.; Yuan, Z. G.; Ni, B. J. Modeling of Simultaneous Anaerobic Methane and Ammonium Oxidation in a Membrane Biofilm Reactor. *Environ. Sci. Technol.* **2014**, *48*, 9540–9547.

(23) Liu, Y. W.; Ngo, H. H.; Guo, W. S.; Peng, L.; Wang, D. B.; Ni, B. J. The roles of free ammonia (FA) in biological wastewater treatment processes: A review. *Environ. Int.* **2019**, *123*, 10–19.

(24) Li, X.; Zhang, W. J.; Xue, S. L.; Lai, S. Z.; Li, J.; Chen, H.; Liu, Z. H.; Xue, G. Enrichment of D-lactic acid from organic wastes catalyzed by zero-valent iron: an approach for sustainable lactate isomerization. *Green Chem.* **2017**, *19*, 928–936.

(25) Xue, G.; Lai, S. Z.; Li, X.; Zhang, W. J.; You, J. G.; Chen, H.; Qian, Y. J.; Gao, P.; Liu, Z. H.; Liu, Y. A. Efficient bioconversion of organic wastes to high optical activity of L-lactic acid stimulated by cathode in mixed microbial consortium. *Water Res.* **2018**, *131*, 1–10.

(26) Zhang, W. J.; Li, X.; Zhang, T.; Li, J.; Lai, S. Z.; Chen, H.; Gao, P.; Xue, G. High-rate lactic acid production from food waste and waste activated sludge via interactive control of pH adjustment and fermentation temperature. *Chem. Eng. J.* **2017**, *328*, 197–206.

(27) Song, K.; Yeerken, S.; Li, L.; Sun, J.; Wang, Q. Improving Post-Anaerobic Digestion of Full-Scale Anaerobic Digestate Using Free Ammonia Treatment. *ACS Sustainable Chem. Eng.* **2019**, *7*, 7171–7176.

(28) Van Ree, K.; Gehl, B.; Chehab, E. W.; Tsai, Y. C.; Braam, J. Nitric oxide accumulation in *Arabidopsis* is independent of NOA1 in the presence of sucrose. *Plant J.* **2011**, *68*, 225–233.

(29) Zhao, J.; Liu, Y.; Wang, Y.; Lian, Y.; Wang, Q.; Yang, Q.; Wang, D.; Xie, G.-J.; Zeng, G.; Sun, Y.; et al. Clarifying the role of free ammonia in the production of short-chain fatty acids from waste activated sludge anaerobic fermentation. *ACS Sustainable Chem. Eng.* **2018**, *6*, 14104–14113.

(30) Wei, W.; Zhou, X.; Wang, D.; Sun, J.; Wang, Q. Free ammonia pre-treatment of secondary sludge significantly increases anaerobic methane production. *Water Res.* **2017**, *118*, 12–19.

(31) Westerholm, M.; Leven, L.; Schnurer, A. Bioaugmentation of Syntrophic Acetate-Oxidizing Culture in Biogas Reactors Exposed to Increasing Levels of Ammonia. *Appl. Environ. Microbiol.* **2012**, *78*, 7619–7625.

(32) Wu, Q.-L.; Guo, W.-Q.; Zheng, H.-S.; Luo, H.-C.; Feng, X.-C.; Yin, R.-L.; Ren, N.-Q. Enhancement of volatile fatty acid production by co-fermentation of food waste and excess sludge without pH control: the mechanism and microbial community analyses. *Bioresour. Technol.* **2016**, *216*, 653–660.

(33) Yan, Y.; Feng, L.; Zhang, C.; Wisniewski, C.; Zhou, Q. Ultrasonic enhancement of waste activated sludge hydrolysis and volatile fatty acids accumulation at pH 10.0. *Water Res.* **2010**, *44*, 3329–3336.

(34) Gao, J. L.; Lv, F. Y.; Wang, X. M.; Yuan, M.; Li, J. W.; Wu, Q. Y.; Sun, J. G. *Flavobacterium endophyticum* sp. nov., a nifH gene harbouring endophytic bacterium isolated from maize root. *Int. J. Syst. Evol. Microbiol.* **2015**, *65*, 3900–3904.

(35) Abdel-Rahman, M. A.; Tashiro, Y.; Zendo, T.; Hanada, K.; Shibata, K.; Sonomoto, K. Efficient homofermentative L-(+)-lactic acid production from xylose by a novel lactic acid bacterium, *Enterococcus mundtii* QU 25. *Appl. Environ. Microbiol.* **2011**, *77*, 1892–1895.

(36) Tashiro, Y.; Inokuchi, S.; Poudel, P.; Okugawa, Y.; Miyamoto, H.; Miyamoto, H.; Sakai, K. Novel pH control strategy for efficient production of optically active L-lactic acid from kitchen refuse using a mixed culture system. *Bioresour. Technol.* **2016**, *216*, 52–59.

(37) Schmidt, V. S.; Mayr, R.; Wenning, M.; Glöckner, J.; Busse, H.-J.; Scherer, S. *Bavariococcus seileri* gen. nov., sp. nov., isolated from the surface and smear water of German red smear soft cheese. *Int. J. Syst. Evol. Microbiol.* **2009**, *59*, 2437–2443.

(38) Xiong, Z.; Hussain, A.; Lee, J.; Lee, H.-S. Food waste fermentation in a leach bed reactor: Reactor performance, and microbial ecology and dynamics. *Bioresour. Technol.* **2019**, *274*, 153–161.

(39) Yu, D. H.; Yang, J. Y.; Teng, F.; Feng, L. L.; Fang, X. X.; Ren, H. J. Bioaugmentation Treatment of Mature Landfill Leachate by New Isolated Ammonia Nitrogen and Humic Acid Resistant Microorganism. *J. Microbiol. Biotechnol.* **2014**, *24*, 987–997.

(40) Liu, X.; Wang, L.; Pang, L. Application of a novel strain *Corynebacterium pollutisoli* SPH6 to improve nitrogen removal in an anaerobic/aerobic-moving bed biofilm reactor (A/O-MBBR). *Bioresour. Technol.* **2018**, *269*, 113–120.

(41) Zheng, Z. J.; Sheng, B. B.; Ma, C. Q.; Zhang, H. W.; Gao, C.; Su, F.; Xu, P. Relative Catalytic Efficiency of IdhL- and IdhD-Encoded Products Is Crucial for Optical Purity of Lactic Acid Produced by *Lactobacillus* Strains. *Appl. Environ. Microbiol.* **2012**, *78*, 3480–3483.

(42) Ye, T.; Li, X.; Zhang, T.; Su, Y.; Zhang, W.; Li, J.; Gan, Y.; Zhang, A.; Liu, Y.; Xue, G. Copper (II) addition to accelerate lactic acid production from co-fermentation of food waste and waste activated sludge: Understanding of the corresponding metabolisms,



microbial community and predictive functional profiling. *Waste Manage* **2018**, 76, 414–422.

(43) Beltran, G.; Esteve-Zarzoso, B.; Rozes, N.; Mas, A.; Guillamon, J. M. Influence of the timing of nitrogen additions during synthetic grape must fermentations on fermentation kinetics and nitrogen consumption. *J. Agric. Food Chem.* **2005**, 53, 996–1002.

(44) Li, X.; Peng, Y.; Ren, N.; Li, B.; Chai, T.; Zhang, L. Effect of temperature on short chain fatty acids (SCFAs) accumulation and microbiological transformation in sludge alkaline fermentation with Ca(OH)(2) adjustment. *Water Res.* **2014**, 61, 34–45.

(45) Wang, Q. L.; Duan, H. R.; Wei, W.; Ni, B. J.; Laloo, A.; Yuan, Z. G. Achieving Stable Mainstream Nitrogen Removal via the Nitrite Pathway by Sludge Treatment Using Free Ammonia. *Environ. Sci. Technol.* **2017**, 51, 9800–9807.

(46) Veuger, B.; Middelburg, J. J.; Boschker, H. T.; Houtekamer, M. Analysis of <sup>15</sup>N incorporation into D-alanine: A new method for tracing nitrogen uptake by bacteria. *Limnol. Oceanogr.: Methods* **2005**, 3, 230–240.

(47) Liu, C. G.; Xue, C.; Lin, Y. H.; Bai, F. W. Redox potential control and applications in microaerobic and anaerobic fermentations. *Biotechnol. Adv.* **2013**, 31, 257–265.

(48) Du, C.; Yan, H.; Zhang, Y.; Li, Y.; Cao, Z. Use of oxidoreduction potential as an indicator to regulate 1,3-propanediol fermentation by *Klebsiella pneumoniae*. *Appl. Microbiol. Biotechnol.* **2006**, 69, 554–563.

(49) Choi, O.; Um, Y.; Sang, B.-I. Butyrate production enhancement by *Clostridium tyrobutyricum* using electron mediators and a cathodic electron donor. *Biotechnol. Bioeng.* **2012**, 109, 2494–2502.

(50) Zhou, M.; Chen, J.; Freguia, S.; Rabaeys, K.; Keller, J. Carbon and electron fluxes during the electricity driven 1,3-propanediol biosynthesis from glycerol. *Environ. Sci. Technol.* **2013**, 47, 11199–11205.

(51) Menzel, K.; Ahrens, K.; Zeng, A. P.; Deckwer, W. D. Kinetic, dynamic, and pathway studies of glycerol metabolism by *Klebsiella pneumoniae* in anaerobic continuous culture: IV. Enzymes and fluxes of pyruvate metabolism. *Biotechnol. Bioeng.* **1998**, 60, 617–626.